Journal of Sound and Vibration (1998) **218**(4), 619–658
Article No. sv981853

COMPOSITE ELEMENT METHOD FOR VIBRATION ANALYSIS OF STRUCTURE, PART I: PRINCIPLE AND C^0 ELEMENT (BAR)

P. ZENG*

Department of Mechanical Engineering, Tsinghua University, Beijing 100084, *P. R. China*

(*Received* 20 *May* 1997, *and in final form* 29 *June* 1998)

A series of two papers is devoted to develop a new kind of numerical method for vibration analysis of structure, called Composite Element Method (CEM), by combining the conventional finite element method and classical analytical theory, aiming at utilizing both the versatility of the traditional FEM and the closed analytical solution of classical theory. First of all, two sets of coordinate systems are defined to describe the displacement field of discretization element: the nodal DOF system (same as in the conventional FEM), as well as the field DOF system of element. The goal of the former is to inherit the versatility of the conventional FEM; the latter is to obtain the higher approximate degree of accuracy. These two sets of coordinate systems are coupled and combined by means of the Rayleigh–Ritz principle. Two kinds of approaches are available to improve the CEM: (1) refining the element mesh, i.e., *h*-version, (2) increasing the degrees of freedom based upon the classical solution (i.e., *c*-DOF), called *c*-version. The numerical results show that *c*-version possesses a potential to lead to a superconvergence. This paper is the first of the series concentrating on the principle of CEM, C^0 element and the related applications.

1. INTRODUCTION

Modern large and precise structures (such as buildings, civil engineering works, spaceshuttles, space stations, aerocraft, trains, automobiles, robotics, antennas, satellites, manipulators, etc.) call for a demand on the accurate dynamic analysis for both lower and higher eigenfrequencies. As to the present situation of finite element technique [1, 2], two main kinds of methods are available to improve the degree of accuracy. The first, and most common, involves refining the finite element mesh whilst keeping the degree of the elements fixed. This is termed the *h*-version of FEM (finite element method) or simply FEM. The second method involves keeping the mesh size constant and letting the degree of the approximating polynomial functions tend to infinity [3]. This approach is better known as the *p*-version of the FEM, or the hierarchical finite element method (HFEM) [4]. Unfortunately, they tend to be either low in efficiency or too complex. For example, the resulting stiffness and mass matrix from densely refining the finite

0022–460X/98/490619 + 40 $30.00/0

element mesh are quite huge. Consequently, very large eigenvalue problems must be solved, with cost computation effort. Also the difficulty of extreme complexity of the p-version or HFEM must be encountered [5, 6]. It is noted that the research on the p-version or the h–p version has not yet been applied in practice. But these topics are arousing the interest of many scientists. Also, some condensed approaches are utilized to reduce the computational effort whilst obtaining a higher accuracy, for instance, the substructural method and the finite strip method, etc.

As we know, some closed analytical solutions for the components with regular geometric shapes and simple boundary conditions can be obtained by the classical theory. These solutions include [7]:

- longitudinal vibration problem of a bar or rod
- torsional vibration problem of a shaft or rod
- lateral transverse vibration problem of a beam
- transverse vibration problem of a membrane
- transverse vibration problem of a thin plate

But these closed analytical solutions are viable only within the scope of some special geometry shapes and supports (i.e. simple–simple, clamped–clamped, free–free, clamped–pinned, etc.). It is therefore desirable to combine the advantages of classical theory and the conventional FEM to get a new finite element with high efficiency and good accuracy. How to implement a combination of these two approaches? The Rayleigh–Ritz principle supplies an important tool. This is because, first, the FEM and the Rayleigh–Ritz principle are essentially equivalent from the viewpoint of variational principle. Secondly, the Rayleigh–Ritz principle is an inclusion principle that permits all admirable-trial solutions satisfying the boundary conditions.

In the papers of this series, a new numerical analytical approach, i.e., Composite Element Method, is proposed which combines the advantages of the FEM and classical theory. More detailedly, the longitudinal bar element (C^0 problem), the torsional shaft element (C^0 problem) as well as the bending beam element (C^1 problem) are addressed. In the Composite Element Method, the approach in which the degrees of freedom are increased based on the classical solution, is called the c-version. It will be found that the c-version of the CEM method can lead to a superconvergence.

2. COMPOSITE ELEMENT METHOD

2.1. PHILOSOPHY OF COMBINING CLASSICAL THEORY AND FEM

From a comparison between the classical approach and FEM in several aspects: the form of solution function, solving procedure, accuracy, efficiency, versatility and applicable scope, etc., we know that both classical theory and FEM possess individual characteristics when being used to solve the differential equations or mechanics problems. So we expect to develop a new method to combine the advantages of these two methods to develop a new method. The first aim of the new method should be to adopt the verticality of the FEM wherein the field

function is expressed in the form of nodal values. The second aim is to embed the analytical solution of classical theory over the domain of the element into the field function of the discretized element. To this end, the first step which must be taken is to define an appropriate coordinate system of element, which is used as a fundamental frame to describe the displacement field of element. Then some attention should be paid to the construction of displacement field based on the given coordinate system. Meanwhile, the related boundary condition of element must be matched. Detailed discussions are presented below.

2.2. NODAL COORDINATE AND FIELD COORDINATE

(1) *Strategy*

As we know, a coordinate system can provide a basic framework within which the displacement field can be built and studied. Based upon the above strategy, we need to construct two coordinate systems, i.e., the nodal coordinate system for adopting the conventional FEM, and the field coordinate system for utilizing the classical theory. A nodal coordinate system utilizes the nodal displacement as the coordinate DOF to describe the displacement field; however, the field coordinate utilizes a set of basis functions obtained from classical theory to describe the displacement field.

For any element, without any loss of generality, we choose the following combination of both the polynomials and the analytical functions to describe the displacement field

$$U(\xi) = \mathbf{N}(\xi)\mathbf{q} + \phi(\xi)\mathbf{c}. \tag{1}$$

It can be seen that $U(\xi)$ is the sum of two parts:

$$U(\xi) = U_{FEM}(\xi) + U_{CT}(\xi) \tag{2}$$

where

$$U_{FEM}(\xi) = \mathbf{N}(\xi)\mathbf{q} \tag{3}$$

$$U_{CT}(\xi) = \phi(\xi)\mathbf{c} \tag{4}$$

where $U_{FEM}(\xi)$ is the displacement field function by FEM based on nodel DOF, $\mathbf{N}(\xi)$ is the space-dependent shape function of the conventional FEM, $U_{CT}(\xi)$ is the displacement field function by the classical theory based on field DOF, $\phi(\xi)$ is the analytical function series by classical theory. According to the above expression, obviously, $\mathbf{q}$ is the nodal coordinate of the conventional FEM, also called nodal DOF, and $\mathbf{c}$ is the field coordinate, also called c-DOF or c-coordinate. It must be pointed out that the field coordinate and its basis function $\phi(\xi)$ is not an arbitrary function; it must satisfy some requirements, especially the boundary conditions of element.

(2) *Displacement field function of FEM*

Equation (1) defines two coordinate systems. One of them is the nodal coordinate system on which we can employ the conventional FEM.

Fundamental to the successful implementation of the FEM is the selection of adequate trial functions for each element. The trial functions are approximate patterns of displacements, rotations, or other fundamental variables often expressed in terms of the same variables at the nodes. Usually, the interpolation polynomials in terms of nodal degrees of freedom [8] are used as the displacement field function of the FEM. To achieve monotonic convergence, this trial function for displacement field must be complete and compatible (or conforming). It means that some convergence requirement must be satisfied.

(3) *Displacement field function by classical theory*

We can solve the differential dynamic equation of element by the classical theory under some special compatible conditions in order to get the expression $U_{CT}(\xi)$ of displacement field function for element.

Assume the solution to be a set of functions:

$$\phi_1(\xi), \phi_2(\xi), \ldots, \phi_n(\xi). \tag{5}$$

A linear combination of them can form the second part $U_{CT}(\xi)$ of the displacement

$$U_{CT}(\xi) = \sum_{r=1}^{n} c_r \phi_r(\xi) \tag{6}$$

where c_r is the coefficients.

Note that the function $\phi_r(\xi)$ is defined over the entire element domain with the special values at the boundary nodes.

- **Coupling boundary condition of element**

In the conventional FEM, the discretized element needs to satisfy only the nodal condition, i.e., the constructed displacement field function of element must be interpolated by the nodal displacement or/and its slope. But this situation has a difference for the displacement field constructed by equation (1). Since the first part (i.e., the interpolation displacement function of FEM) $\mathbf{N}(\xi)\mathbf{q}$ has already satisfied the nodal conditions of element, the second part $\phi(\xi)\mathbf{c}$ should satisfy some other admissible conditions. We call the conditions, which the second part $\phi(\xi)\mathbf{c}$ must obey, the boundary condition of element. In other words, it means that if we utilize the analytical result of classical theory to build the displacement field function of element [i.e., second part of equation (1)], this analytical result is not arbitrary, but must obey some boundary conditions.

Obviously, in a straightforward manner, we know that the displacement field $U(\xi)$ of element must satisfy the nodal condition, and if the first part $\mathbf{N}(\xi)\mathbf{q}$ of displacement field $U(\xi)$ takes the interpolation polynomial function of the conventional FEM, it can be found that $\mathbf{N}(\xi)\mathbf{q}$ has already satisfield these nodal conditions. Therefore the second part $U_{CT}(\xi)$ of $U(\xi)$ must obey zero-displacement and coupling slope conditions at the nodes of element, which are the boundary conditions of element when using the analytical results of the classical theory stated above.

For the C^0 continuous problem, the coupling boundary conditions are

$$\phi_r(\xi)|_{\xi=0} = 0, \qquad \phi_r(\xi)|_{\xi=1} = 0 \quad r = 1, 2, 3, \ldots \tag{7}$$

For the C^1 continuous problem, the coupling boundary conditions are

$$\phi_r(\xi)|_{\xi=0} = 0, \qquad \phi_r(\xi)|_{\xi=1} = 0$$

$$\left.\frac{\mathrm{d}\phi_r(\xi)}{\mathrm{d}\xi}\right|_{\xi=0} = 0, \qquad \left.\frac{\mathrm{d}\phi_r(\xi)}{\mathrm{d}\xi}\right|_{\xi=1} = 0 \quad r = 1, 2, 3, \ldots. \tag{8}$$

Arbitrarily, for the C^k continuous problem, the coupling boundary conditions are

$$\phi_r(\xi)|_{\xi=0} = 0, \qquad \phi_r(\xi)|_{\xi=1} = 0$$

$$\left.\frac{\mathrm{d}\phi_r(\xi)}{\mathrm{d}\xi}\right|_{\xi=0} = 0, \qquad \left.\frac{\mathrm{d}\phi_r(\xi)}{\mathrm{d}\xi}\right|_{\xi=1} = 0$$

$$\vdots \qquad\qquad \vdots$$

$$\left.\frac{\mathrm{d}^k\phi_r(\xi)}{\mathrm{d}\xi^k}\right|_{\xi=0} = 0, \qquad \left.\frac{\mathrm{d}^k\phi_r(\xi)}{\mathrm{d}\xi^k}\right|_{\xi=1} = 0 \quad r = 1, 2, 3, \ldots. \tag{9}$$

Note that the coupling boundary conditions of element will be very important because they are used as the boundary conditions when we solve the differential vibration equation by the classical theory in order to obtain the analytical form of the second part $\phi_r(\xi)$ of $U(\xi)$. Moreover, fortunately, in most cases, the $\phi_r(\xi)$ under simply supported boundary conditions can be exactly obtained by solving the differential equation of classical theory under the coupling boundary conditions.

- **Trial functions under the coupling boundary condition**

In structural engineering, longitudinal bar, torsional shaft and bending beam are the basic components. Obviously, longitudinal bar and torsional shaft belong to the C^0 problem, and bending beam belongs to the C^1 problem. Their exact analytical solutions under the coupling boundary conditions are presented below [9].

(1) C^0 *problem* (*longitudinal bar*)

As discussed above, the Composite Element Method requires the analytical solution under the coupling boundary conditions of a longitudinal bar, i.e.,

$$U(x)|_{x=0} = 0, \qquad U(x)|_{x=l} = 0 \tag{10}$$

where $U(x)$ is the longitudinal displacement.

Actually, this is the case of the clamped–clamped bar. The corresponding solution can be obtained as

$$U_r(x) = c_r \sin \beta_r x \quad r = 1, 2, 3, \ldots. \tag{11}$$

where

$$\beta_r = r\frac{\pi}{l}. \tag{12}$$

Here c_r are a set of constants. Finally, the solution function $u(x, t)$ is given as from equation (11)

$$\begin{aligned} u(x, t) &= U_r(x) \cdot G_r(t) \\ &= c_r \sin \beta_r x \cdot \sin \omega_r t \quad r = 1, 2, 3, \ldots \end{aligned} \tag{13}$$

where

$$\omega_r^2 = \frac{E}{\rho}\beta_r^2. \tag{14}$$

E is the Young's modulus and ρ is the density.

Note that $U_r(x)$ are a set of natural mode shape functions, which will be combined or embedded into the displacement field of bar element in Composite Element Method together with the interpolation polynomial function of the conventional FEM.

(2) C^0 *problem* (*torsional shaft*)

The Composite Element Method requires the analytical solution under the coupling boundary conditions for a torsional shaft, i.e.,

$$\Theta(x)|_{x=0} = 0, \qquad \Theta(x)|_{x=l} = 0 \tag{15}$$

where $\Theta(x)$ is the torsional displacement.

Similarly, this is the case of the clamped–clamped shaft. The corresponding solution can be found as

$$\Theta_r(x) = c_r \sin \beta_r x, \quad r = 1, 2, 3, \ldots \tag{16}$$

where

$$\beta_r = r\frac{\pi}{l} \tag{17}$$

Here c_r are a set of constants. Finally, the solution $\vartheta(x, t)$ is given by

$$\begin{aligned} \vartheta(x, t) &= \Theta_r(x) \cdot G_r(t) \\ &= c_r \sin \beta_r x \cdot \sin \omega_r t, \quad r = 1, 2, 3, \ldots \end{aligned} \tag{18}$$

where

$$\omega_r^2 = \frac{G}{\rho}\beta_r^2. \tag{19}$$

G is the shear modulus and ρ is the density.

Note that $\Theta_r(x)$ are a set of natural mode shape functions, which will be combined or embedded into the displacement field of torsional element in Composite Element together with the interpolation polynomial function of the conventional FEM.

2.3. CONVERGENCE OF COMPOSITE ELEMENT METHOD

Presumably, for successful finite element solutions (including composite element), the displacement trial functions should lead to an analysis that monotonically converges to the exact solution as the size of the elements tends to zero [10], i.e., the accuracy of the solution increases as the element mesh is continuously refined. To achieve monotonic convergence, the element must be complete and compatible (or conforming). The requirement for completeness means that the displacement functions must be able to represent the rigid body displacements and constant strain states [11]. Compatibility assures that no gaps occur within the elements and between the elements when the system of elements is assembled and loaded [11].

Below we discuss the completeness and compatibility of the Composite Element Method.

(1) *Completeness of composite element*

The trial function of Composite Element is composed of two parts, one of which is the nodal interpolation function of the conventional FEM. If it satisfies the requirement for completeness, we can say that the trial function of CEM combined by FEM and classical theory is sure to be complete, and is able to represent the rigid displacement and constant strain, which will be verified in the numerical examples later.

(2) *Compatibility of composite element*

To satisfy the condition of compatibility, the trial functions should be chosen such that (a) they are continuous within the element, and (b) at the element interfaces at least the first k derivatives are continuous, where $(k + 1)$ is the highest appearing in the functional of the principle of virtual work, i.e., the highest derivative appearing in the strain-displacement matrix $\mathbf{B}(x)$. Trial functions are said to exhibit C^k continuity if their derivatives of order k are continuous. Obviously, a longitudinal bar element and a torsional shaft element belong to the sort of C^0 continuity, and a bending beam element belongs to the sort of C^1 continuity. For a longitudinal bar element, a torsional shaft element and a bending beam element of CEM, we can verify that they all satisfy the compatibility requirement. The reason is that the trial function of CEM has two parts: one part comes from the conventional FEM which meets the compatibility requirement and the other is the analytical solution of classical theory under the special compatible boundary conditions which possesses the derivative of arbitrary order and also meets all compatibility requirements.

(3) *h-version and c-version of composite element*

To obtain a higher accuracy, two approaches are available to improve the CEM:

- Refining the element mesh, i.e., h-version.
- Increasing the degrees of freedom based on the classical solutions (i.e., c-DOF), called c-version.

Further discussions can show that the *h*-version of CEM is completely similar to the conventional FEMs, but the *c*-version of the CEM is not entirely similar to the *p*-version of the conventional FEM because each basis function in CEM is obtained by the analytical solution of classical theory which is a continuous function with the arbitrary order of continuous derivative, not a polynomial. So, the *c*-version of the Composite Element Method can improve the accuracy and efficiency with less computation effort. It is especially true for the computation of eigenvalue and eigenvector in structural dynamics. It will be found that the Composite Element Method possesses a possibility to lead to a superconvergence. In the following sections, a large number of numerical examples will confirm this.

2.4. PHYSICAL INTUITION OF COMPOSITE ELEMENT METHOD

As we know, the discretization of a continuous problem has been approached differently by the mathematician and the engineer. The former has developed general techniques applicable directly to differential equations governing the problem, such as finite difference approximation, various weighted residual procedures, or approximate techniques of determining the stationary of a properly defined 'functional'. The engineer, on the other hand, often approaches the problem more intuitively by creating an analogy between real discrete elements and finite portions of a continuum domain. For instance, in the field of solid mechanics, [12–14], in the early forties, showed that a reasonably good solution to an elastic continuum problem could be obtained by substituting small portions of the continuum by an arrangement of simple elastic bars. Later, in the same context, Argyris [15] and Turner *et al*. [16] showed that a more direct, but no less intuitive, substitution of properties could be made much more directly by considering that small portions or 'elements' in a continuum behave in a simplified manner.

It is from the engineering 'direct analogy' view that the term 'finite element' has been born. Clough [17] appears to be the first to use this term, which implies a direct use of standard methodology applicable to discrete systems. Conceptually and as well as from the computational viewpoint, this is of utmost importance. The first allows an improved understanding to be obtained, the second the use of a unified approach to the variety of problems and the development of standard computational procedures. Since the early sixties much progress has been made, and today the purely mathematical and 'analogy' approaches are fully reconciled.

The Composite Element Method developed by the series of papers has a situation completely similar to finite element both intuitively and mathematically. First, the Composite Element Method has the same physical discretization as FEM, and all analyses follow a standard procedure which is universally adaptable to discrete systems. Second, an inclusion principle, i.e., the Rayleigh–Ritz principle, is mathematically utilized to construct the displacement function of element. Theoretically, the Composite Element can include the conventional finite element; in other words, the conventional finite element is a special case of Composite Element wherein the field coordinate based upon the classical theory (i.e., *c*-DOF) is neglected (a related discussion is presented below).

2.5. COMPOSITE ELEMENT METHOD AND FINITE ELEMENT METHOD

According to the philosophy of constructing Composite Element, from equation (2), if we let $\mathbf{c} = 0$ (i.e., c-DOF is neglected), in field function of element will be

$$U(\xi) = U_{FEM}(\xi)$$

$$= \mathbf{N}(\xi) \cdot \mathbf{q}. \tag{20}$$

Obviously, it is the field function of the conventional FEM. In this case, the composite element is reduced as a conventional finite element.

Now we give some comments on the comparisons between CEM, p-version of FEM and HFEM (hierarchical FEM).

(1) *The conventional finite element method*

The basic idea of FEM is piecewise approximation. The functions used to represent the behavior of the solution within an element are called interpolation functions or approximating models. Polynomial type of interpolation functions have been most widely used in the literature.

Theoretically a polynomial of infinite order corresponds to the exact solution. But in practice we take polynomials of finite or only as an approximation. Although trigonometric functions also possess some of these properties, they are seldom used in the finite element analysis [11].

There are two main ways to improve the accuracy of the conventional FEM. The first, and most common, involves refining the element mesh whilst keeping the order of the interpolation polynomials of element fixed. This is termed the h-version of the FEM or simply the FEM. The second method involves keeping the mesh size constant and increasing the order of the interpolation polynomial. This approach is better known as the p-version of the FEM. The well known hierarchical finite element method (HFEM) is one of the p-versions. In recent years the adaptive methods have come to be the focus of interest. Various papers [18–21] address the equations of adaptive approaches in the FEM. In two dimensional adaptive research code FEARS [22] and PLTMG [23] are available. Both codes deal with the h-version and linear ($p = 1$) elements. However, there is no adaptive h–p version code and only little work has been done addressing this question.

The goals in a successful adaptive h–p version are twofold: (a) the method should lead to a discretization that corresponds to a solution with a specified accuracy and (b) this should be accomplished in a minimum number of steps with a minimum number of unknowns. Such a mesh is termed 'optimal'.

But it must be pointed out that since the p-version of FEM is based upon adding inner nodes of element and taking a higher order of polynomial, some computational difficulty and error may occur.

(2) *CEM and p-version of FEM*

In CEM, the bases functions of c-DOF, i.e., higher order functions, come from the exact or near-exact analytical solution under some conditions. Generally, these

are trigonometric functions with excellent mathematical properties. Also the bases functions show an independence on the nodes and are provided with the nature of hierarchical spectra.

As to p-version of FEM, the bases functions come from the higher order interpolation functions in terms of nodes (corner nodes plus additional nodes). Generally, these functions have the form of higher order polynomials. So, they tend to be either low in efficiency or too complex in terms of numerical treatment (especially in calculation of integration), or they may even fail due to large errors in numerical computing.

(3) *CEM and HFEM*

The nature of hierarchical spectra is included in the bases functions of CEM since they are chosen from the exact or near-exact analytical solution under some compatible conditions. Generally, they have the form of trigonometric series. Therefore it would be a merit to carry out the calculation of integration conveniently and exactly. Especially in the development of isoparametric element, CEM will show some good numerical properties.

As to HFEM, the hierarchical bases functions are derioved from Rodrigue's form of Legendre orthogonal polynomials. Generally, these polynomials are complicated. It would be very difficult to treat them on a large scale (especially in the calculations of integrations). Moreover, it could bring about larger calculation errors. Maybe it is one of the reasons that HFEM is not popularly applied in practice so far.

The so-called CEM is, actually, a new type of FEM which combines the versatility of the conventional FEM and the high accuracy of the classical analytical method. Here, composite means combining or coupling. So CEM inherits the excellent properties of h-version, p-version and hierarchical FEM, and has a perfect theoretical foundation. It can be found that CEM could be reduced to a traditional FEM or HFEM with some simplified treatment (e.g., neglecting c-DOF). In other words, a conventional FEM or HFEM (including h-version and p-version) can be considered as a special case of CEM under some conditions. It is desired that CEM become a potential and general method in future with further development.

2.6. STIFFNESS MATRIX AND CONSISTENT MASS MATRIX

From the above discussion, we know that the displacement field of element consists of two parts, i.e.,

$$\begin{aligned} U(\xi) &= U_{FEM}(\xi) + U_{CT}(\xi) \\ &= \mathbf{N}(\xi)\mathbf{q} + \phi(\xi)\mathbf{c} \\ &= \mathbf{S}(\xi) \cdot \delta \end{aligned} \tag{21}$$

where

$$\begin{aligned}\mathbf{S}(\xi) &= [\mathbf{N}(\xi) \quad \phi(\xi)] \\ \delta &= [\mathbf{q}^{\mathrm{T}} \ \mathbf{c}^{\mathrm{T}}] \\ &= [q_1 \ q_2 \ c_1 \ c_2 \cdots c_n]^{\mathrm{T}}. \end{aligned} \tag{22}$$

The function matrix $\mathbf{S}(\xi)$ is defined as the generalized shape function matrix of CEM which consists of both the shape function $\mathbf{N}(\xi)$ of the conventional FEM and the mode shape $\phi(x)$ of the analytical solution of classical theory. The vector δ is called the generalized coordinates (or DOF) of CEM which consists of both the nodal DOF $\mathbf{q}$ of the conventional FEM and the mode coordinate $\mathbf{c}$ of the analytical solution of classical theory.

From equation (21), the strain ε can be expressed as

$$\begin{aligned}\varepsilon &= [\partial]U(\xi) \\ &= [\partial]\mathbf{S}(\xi) \cdot \delta = \mathbf{B}(\xi) \cdot \delta \end{aligned} \tag{23}$$

where

$$\begin{aligned}\mathbf{B}(\xi) &= [\partial]\mathbf{S}(\xi) \\ &= [\partial][\mathbf{N}(\xi) \quad \phi(\xi)] \end{aligned} \tag{24}$$

is called the generalized strain–displacement matrix of CEM which is also composed of two parts: the one of the conventional FEM and the one of classical theory. $[\partial]$ is the operator of strain–displacement relation.

Having the generalized shape function matrix $\mathbf{S}(\xi)$ and the generalized strain–displacement matrix $\mathbf{B}(\xi)$, it is easy to derive the stiffness matrix $\mathbf{k}^e$ and mass matrix $\mathbf{m}^e$ of CEM by the general procedure of the conventional FEM, i.e.,

$$\mathbf{k}^e = \int_V \mathbf{B}^{\mathrm{T}}\mathbf{D}\mathbf{B} \, \mathrm{d}V \tag{25}$$

$$\mathbf{m}^e = \int_V \rho \mathbf{S}^{\mathrm{T}}\mathbf{S} \, \mathrm{d}V \tag{26}$$

where $\mathbf{D}$ is the elastic matrix, and the superscript e denotes each element.

2.7. IMPLEMENTATION PROCEDURE OF COMPOSITE ELEMENT METHOD

The implementation procedure of Composite Element Method is completely similar to that of the conventional FEM, except for introducing c-DOF into the displacement field of element. As to the displacement field of element, we already have a standard way to describe it [see equation (2)]. The corresponding stiffness and mass matrices with an arbitrary c-DOF number will be derived later. So, all implementation procedure can completely follow that of the conventional FEM, such as, the assemblage of element matrices, the treatment of boundary conditions, the solution of global equation, etc. Also the Composite Element Method can be completely inlaid into the present FEM software with less programming effort (see Figure 1).

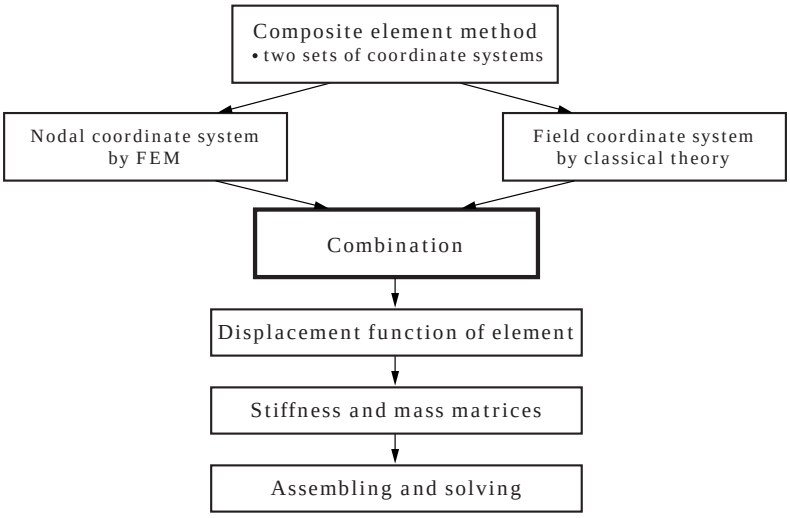

Figure 1. Implementation procedure of CEM.

3. C^0 ELEMENTS

3.1. DISPLACEMENT OF LONGITUDINAL BAR ELEMENT

Consider the pin-jointed bar element shown in Figure 2 where the local x-axis is taken in the axial direction of the element with its origin at the corner (or local node) 1.

$$U(x) = U_{FEM}(x) + U_{CT}(x). \tag{27}$$

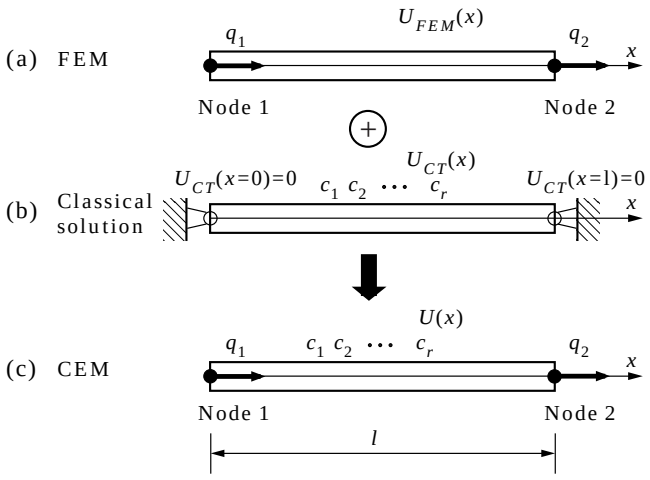

Figure 2. Constructing of CEM for longitudinal bar.

From the above discussion, we can construct the displacement function $U(x)$ as

$$\begin{aligned} U(x) &= U_{FEM}(x) + U_{CT}(x) \\ &= \left(1 - \frac{x}{l}\right) q_1 + \frac{x}{l} q_2 + c_1 \sin \beta_1 x + c_2 \sin \beta_2 x + \cdots + c_n \sin \beta_n x \\ &= \left(1 - \frac{x}{l}\right) q_1 + \frac{x}{l} q_2 + c_1 \sin \pi \frac{x}{l} + c_2 \sin 2\pi \frac{x}{l} + \cdots + c_n \sin n\pi \frac{x}{l} \\ &= \mathbf{N}(x)\mathbf{q} + \phi(x)\mathbf{c} \\ &= \mathbf{S}(x) \cdot \delta \end{aligned} \tag{28}$$

where

$$\begin{aligned} \mathbf{S}(x) &= [\mathbf{N}(x) \quad \phi(x)] \\ &= \left[\left(1 - \frac{x}{l}\right) \quad \frac{x}{l} \quad \sin \pi \frac{x}{l} \quad \sin 2\pi \frac{x}{l} \quad \cdots \quad \sin n\pi \frac{x}{l}\right] \end{aligned} \tag{29}$$

$$\begin{aligned} \delta &= [\mathbf{q}^{\mathrm{T}} \quad \mathbf{c}^{\mathrm{T}}] \\ &= [q_1 \quad q_2 \quad c_1 \quad c_2 \quad \cdots \quad c_n]^{\mathrm{T}}. \end{aligned} \tag{30}$$

From equation (28), the axial strain can be expressed as

$$\begin{aligned} \varepsilon &= \frac{\partial U(x)}{\partial x} \\ &= \frac{\partial \mathbf{S}(x)}{\partial x} \cdot \delta = \mathbf{B}(x) \cdot \delta \end{aligned} \tag{31}$$

where

$$\begin{aligned} \mathbf{B}(x) &= \frac{\partial \mathbf{S}(x)}{\partial x} \\ &= \left[-\frac{1}{l} \quad \frac{1}{l} \quad \frac{\pi}{l} \cos \pi \frac{x}{l} \quad \frac{2\pi}{l} \cos 2\pi \frac{x}{l} \quad \cdots \quad \frac{n\pi}{l} \cos n\pi \frac{x}{l}\right] \end{aligned} \tag{32}$$

is called the generalized strain–displacement matrix of CEM which is also composed of two parts: the one of the conventional FEM and the one of classical theory.

When the generalized shape function matrix $\mathbf{S}(x)$ and the generalized strain–displacement matrix $\mathbf{B}(x)$ are available, it is easy to derive the stiffness matrix $\mathbf{k}^e$ and mass matrix $\mathbf{m}^e$ of Composite Element by the general procedure of the conventional FEM.

3.2. STIFFNESS MATRIX AND MASS MATRIX

Now we derive the formulation in local coordinates. As discussed above, the displacement field function $U(x)$ in the one dimensional case (longitudinal bar) is expressed by equation (27). So, the matrix $\mathbf{S}(x)$ of shape function and the matrix $\mathbf{B}(x)$ of strain–displacement relation can be found from equations (29) and (32) respectively. Further, we can calculate the stiffness matrix $\mathbf{k}^e$ of element according to the expression (25) as

$$\mathbf{k}^e = \frac{EA}{l} \cdot \begin{array}{c} \begin{array}{cccccccc} q_1 & q_2 & c_1 & c_2 & \cdots & \cdots & c_r & \end{array} \\ \left[\begin{array}{cc|ccccc} 1 & -1 & & & & & & \\ -1 & 1 & & & & 0 & & \\ \hline & & \frac{\pi^2}{2} & & & & & \\ & & & \frac{4\pi^2}{2} & & 0 & & \\ & 0 & & & \ddots & & & \\ & & & 0 & & \ddots & & \\ & & & & & & \frac{r^2\pi^2}{2} & \end{array}\right] \end{array} \begin{array}{c} q_1 \\ q_2 \\ \\ c_1 \\ \\ c_2 \\ \vdots \\ \vdots \\ \\ c_r \end{array} \tag{33}$$

Similarly, from the expression (26) the consistent mass matrix $\mathbf{m}^e$ of element is given as

$$\mathbf{m}^e = \rho A l \cdot \begin{array}{c} \begin{array}{cccccccc} q_1 & q_2 & c_1 & c_2 & \cdots & \cdots & c_r & \end{array} \\ \left[\begin{array}{cc|ccccc} \frac{1}{3} & \frac{1}{6} & & & & & & \\ \frac{1}{6} & \frac{1}{3} & & & \textit{symmetric} & & & \\ \hline \frac{1}{\pi} & \frac{1}{\pi} & \frac{1}{2} & & & & & \\ \frac{1}{2\pi} & -\frac{1}{2\pi} & & \frac{1}{2} & & 0 & & \\ \vdots & \vdots & & \ddots & & & & \\ \vdots & \vdots & & 0 & & \ddots & & \\ \frac{1}{r\pi} & \frac{(-1)^{r+1}}{r\pi} & & & & & \frac{1}{2} & \end{array}\right] \end{array} \begin{array}{c} q_1 \\ q_2 \\ \\ c_1 \\ c_2 \\ \vdots \\ \vdots \\ c_r \end{array} \tag{34}$$

Note that the generalized coordinate δ^e is composed of two parts: the nodal coordinate $\mathbf{q}$ (or nodal DOF) and the c-coordinate (or c-DOF) $\mathbf{c}$:

$$\delta^e = [q_1 \quad q_2 \quad c_1 \quad c_2 \quad \cdots \quad c_r]^{\mathrm{T}}. \tag{35}$$

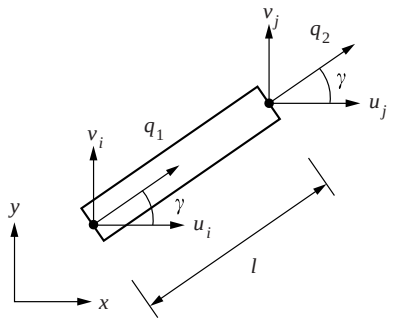

Figure 3. Coordinate transformation in planar case.

Stiffness and mass matrices of the longitudinal bar element in the Composite Element Method possess same properties as those of the conventional FEM [3], i.e.,

(1) Both the stiffness matrix and the mass matrix are symmetric.
(2) The stiffness matrix in the Composite Element Method is positive semi-definite. Also, after elimination of rigid body motion, a stiffness matrix will be positive definite.
(3) The diagonal elements of both stiffness matrix and mass matrix are always positive.

3.3. COORDINATE TRANSFORMATION

As we know, the element characteristic matrices are derived in the local coordinate system suitably oriented for minimizing computational effort. However, the local coordinate systems may be different for different elements. In such a case, before the element equations can be assembled, it is necessary to transform the element equations derived in local coordinate systems so that all the elemental equations are referred to a common global coordinate system.

In order to find the stiffness matrix and the mass matrix of the bar element of the Composite Element Method in the global coordinate system, we need to search the transformation matrix. Let a transformation matrix $\mathbf{T}^e$ exist between the local and the global coordinate systems such that

$$\delta^e = \mathbf{T}^e \bar{\delta}^e \tag{36}$$

where $\bar{\delta}^e$ is the generalized coordinates in the global coordinate system. Now, we use superscript e to indicate each element. The stiffness matrix $\mathbf{K}^e$ and the mass matrix $\mathbf{M}^e$ of the element corresponding to the global coordinate system are given as [11]

$$\mathbf{K}^e = \mathbf{T}^{eT} \mathbf{k}^e \mathbf{T}^e \tag{37}$$

$$\mathbf{M}^e = \mathbf{T}^{eT} \mathbf{m}^e \mathbf{T}^e \tag{38}$$

(1) *Planar case*

Let the (local) nodes 1 and 2 of the bar element correspond to nodes i and j respectively of the global system as shown in Figure 3.

The local displacements q_1 and q_2 can be resolved into components u_i, v_i and u_j, v_j parallel to the global x, y axes respectively. The two sets of displacements are related as

$$q_1 = u_i \cos\gamma + v_i \sin\gamma \tag{39}$$

$$q_2 = u_j \cos\gamma + v_j \sin\gamma \tag{40}$$

where γ is the angle between the line ij and the direction ox. According to the transformation relations (39) and (40), from equation (27) the displacement field of the element can be written as

$$\begin{aligned} U(x) &= \mathbf{S}^e(x)\delta^e \\ &= \left(1 - \frac{x}{l}\right) q_1 + \frac{x}{l} q_2 + \sum_{r=1}^{n} c_r \sin r\pi \frac{x}{l} \\ &= \left(1 - \frac{x}{l}\right)(u_i \cos\gamma + v_i \sin\gamma) + \frac{x}{l}(u_j \cos\gamma + v_j \sin\gamma) + \sum_{r=1}^{n} c_r \sin r\pi \frac{x}{l} \\ &= \mathbf{S}^e(x)\mathbf{T}^e\overline{\delta}^e \end{aligned} \tag{41}$$

where

$$\mathbf{S}^e(x) = \left[\left(1 - \frac{x}{l}\right) \quad \frac{x}{l} \quad \sin\pi\frac{x}{l} \quad \sin 2\pi\frac{x}{l} \quad \cdots \quad \sin n\pi\frac{x}{l}\right] \tag{42}$$

is the shape function matrix,

$$\mathbf{T}^e = \begin{array}{c} \begin{array}{ccccccccc} u_i & v_i & u_j & v_j & c_1 & c_2 & \cdots & \cdots & c_r \end{array} \\ \left[\begin{array}{cccc|ccccc} l_{ij} & m_{ij} & 0 & 0 & & & & & \\ 0 & 0 & l_{ij} & m_{ij} & & 0 & & & \\ \hline & & & & 1 & & & & \\ & & & & & 1 & & 0 & \\ & & & & & & \ddots & & \\ & & 0 & & & 0 & & \ddots & \\ & & & & & & & & 1 \end{array}\right] \end{array} \begin{array}{c} q_1 \\ q_2 \\ c_1 \\ c_2 \\ \vdots \\ \vdots \\ c_r \end{array} \tag{43}$$

is the transformation matrix,

$$\overline{\delta}^e = [u_i \quad v_i \quad u_j \quad v_j \quad c_1 \quad c_2 \quad \cdots \quad c_r]^{\mathrm{T}} \tag{44}$$

is the generalized coordinates in the global coordinate system, and l_{ij}, m_{ij} denote the direction cosines of angles between the line ij and the directions ox, oy, respectively. The direction cosines can be computed in terms of the global coordinates of nodes i and j as

$$l_{ij} = \cos\gamma = \frac{x_j - x_i}{l}, \qquad m_{ij} = \sin\gamma = \frac{y_j - y_i}{l} \tag{45}$$

where (x_i, y_i) and (x_j, y_j) are the global coordinates of nodes i and j respectively, and l is the length of the element ij given by

$$l = \sqrt{(x_j - x_i)^2 + (y_j - y_i)^2}\,. \tag{46}$$

With the help of the expression of transformation matrix (43), we can compute the stiffness and mass matrices in the global coordinate system with equations (37) and (38).

(2) *Spatial case*

In a similar manner, we can derive the same transformatioin relations in the spatial case as shown in equation (36), but here the $\mathbf{T}^e$ matrix is given by

$$\mathbf{T}^e = \begin{array}{c} \begin{array}{cccccccccccc} u_i & v_i & w_i & u_j & v_j & w_j & c_1 & c_2 & \cdots & \cdots & c_r & \end{array} \\ \left[\begin{array}{cccccc|ccccc} l_{ij} & m_{ij} & n_{ij} & 0 & 0 & 0 & & & & & & \\ 0 & 0 & 0 & l_{ij} & m_{ij} & n_{ij} & & 0 & & & & \\ \hline & & & & & & 1 & & & & & \\ & & & & & & & 1 & & 0 & & \\ & & & & & & & & \ddots & & & \\ & & & 0 & & & & 0 & & \ddots & & \\ & & & & & & & & & & 1 & \end{array}\right] \end{array} \begin{array}{c} q_1 \\ q_2 \\ c_1 \\ c_2 \\ \vdots \\ \vdots \\ c_r \end{array} \tag{47}$$

The direction cosines can be computed in terms of the global coordinates of nodes i and j as

$$l_{ij} = \frac{x_j - x_i}{l}, \qquad m_{ij} = \frac{y_j - y_i}{l}, \qquad n_{ij} = \frac{z_j - z_i}{l} \tag{48}$$

where (x_i, y_i, z_i) and (x_j, y_j, z_j) are the global coordinates of i and j respectively, and l is the length of the element ij given by

$$l = \sqrt{(x_j - x_i)^2 + (y_j - y_i)^2 + (z_j - z_i)^2}. \tag{49}$$

From the components of the coordinate transformation matrix (43) and (47), we can find that the transformation is carried out only for the nodal coordinate, and not for the c-coordinate. The reason for this is that the c-coordinate is always defined in the local coordinate system with a closed form, contributes only to the internal displacement field of the element and does not therefore influence its edge displacements. Since the transformation matrix $\mathbf{T}^e$ is the matrix of direction cosines relating the two coordinate systems, it is orthogonal.

3.4. TORSIONAL SHAFT ELEMENT

Similar to the longitudinal bar element, a torsional shaft element belongs to the C^0 continuity problem. So it has the same formulations of stiffness matrix, mass matrix and transformation matrix as the longitudinal bar element.

4. NUMERICAL VERIFICATIONS

4.1. A CLAMPED-FREE ROD

Now, we give a detailed validation for the Composite Element Method, using a clamped-free rod as an example. The contents include: discretizations of 1, 2 as well as 4 elements, effect of the number of c-DOF, and effect of the allocation of c-DOF.

Consider the longitudinal vibration of a clamped-free rod as shown in Figure 4(a). L is the length of the rod, ρ, E are the mass density and Young's modulus respectively. Now, we idealize this bar into 1 element, 2 elements, and 4 elements, and then apply the Composite Element Method to calculate the natural frequencies.

Let

$$\lambda_i^2 = \frac{\rho L^2}{E}\omega_i^2, \quad i = 1, 2, \ldots \tag{50}$$

where ω_i is the natural frequencies. We present the results below.

(1) *Discretization of* 1 *element*

If we take total rod as 1 bar element, then consider several calculating schemes wherein 1c-DOF, 3c-DOF, 7c-DOF, 11c-DOF and 15c-DOF are chosen. Various orders of eigenvalues λ_i^2 are presented in Table 1, in comparison with the exact solutions.

From the results shown in Table 1, we can see that the resultant eigenvalues from λ_1^2 to λ_n^2 (here n is the number of the c-DOF), i.e., within the scope of c-DOF number in each scheme, are very close to the exact solutions (maximum relative error $<3\%$). For example, in the scheme of CEM ($1 \times 15c$), i.e., using one CEM element with 15c-DOF, the total-DOF is 16 (i.e., c-DOF plus nodal DOF), the resultant eigenvalues from λ_1^2 to λ_{15}^2 are close to the exact solutions, and the maximum relative error (i.e., for λ_{15}^2) only reaches 2·12%.

(2) *Discretization of* 2 *elements*

Now, we idealize this clamped-free rod into 2 elements [shown in Figure 4(b)]. Consider several calculating schemes wherein FEM, 1c-DOF, 3c-DOF, 5c-DOF, 7c-DOF are chosen. Various orders of eigenvalues λ_i^2 in various schemes are presented in Table 2, which are compared with the exact solutions.

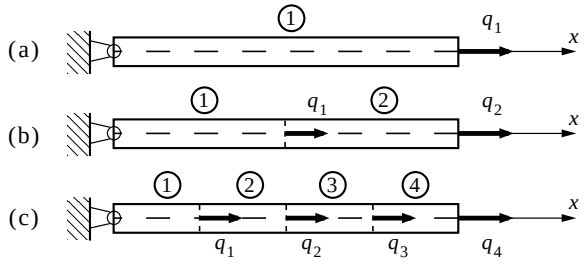

Figure 4. A clamped-free rod and its discretization (in three schemes).

The results of Table 2 also show that the calculated eigenvalues from λ_1^2 to λ_n^2 within the scope of c-DOF number in each scheme approximate to the exact solutions (maximum relative error $<5\%$). For instance, in scheme of CEM ($2 \times 7c$), i.e., using two CEM elements with 7 c-DOF, the total-DOF is 16 (i.e., c-DOF plus nodal DOF), the resulted eigenvalues from λ_1^2 to λ_{14}^2 are very close to the exact solutions, and the maximum relative error (i.e., for λ_{14}^2) only reaches 3·38%.

Obviously, a comparison of Tables 1 and 2 shows that, in the case of the same computational efforts used, the results of the scheme with 2 elements discretization are not better than these with 1 element discretization.

(3) *Discretization of* 4 *elements*

Here, we idealize this clamped-free rod into 4 elements shown in Figure 4(c), and also consider several calculating schemes: FEM, 1c-DOF, 2c-DOF, 3c-DOF. Various orders of eigenvalues λ_i^2 in various schemes are presented in Table 3, which are compared with the exact solutions.

The results of Table 3 also show that the calculated eigenvalues from λ_1^2 to λ_n^2 within the scope of c-DOF number in each scheme very accurately approximate to the exact solutions (maximum relative error $<5{\cdot}5\%$). For instance, in the scheme of CEM ($4 \times 3c$), i.e., using four CEM elements with 3 c-DOF, the total-DOF is 16 (i.e., c-DOF plus nodal DOF), the resultant eigenvalues from λ_1^2 to λ_{12}^2 are very close to the exact solutions, the maximum relative error (i.e., for λ_{12}^2) only reaching 4.62%.

Obviously, a comparison of Tables 1, 2 and 3 shows that, in the case of an equal amount of effort, the results of a scheme with 4 elements discretization (including c-DOF) are not better than those with 1 or 2 element discretization.

(4) *Effect of number of c-DOF*

If we fix the number of total DOF as 8, then consider several schemes: CEM ($1 \times 7c$) (i.e., total c-DOF is 7), CEM ($2 \times 3c$) (i.e., total c-DOF is 6), CEM ($4 \times 1c$) (i.e., total c-DOF is 4), FEM (i.e., total c-DOF is 0). The purpose is to investigate the effect of number of c-DOF on eigenvalues with the computational effort remaining the same. The detailed computational results and comparisons between them are presented in Table 4.

From Table 4, we find that the accuracy achieved by the Composite Element is greatly superior to that by the conventional FEM. Moreover, the scheme with more c-DOF is superior to that with less c-DOF. Note that the above comparison is based on the same amount of computational effort used (i.e., total-DOF of each scheme is 8). We compare the errors of each scheme with the exact solution: as to λ_7^2, the relative error of the CEM ($1 \times 7c$) scheme is 2·88%, and the error of the FEM (8e) scheme already reaches 44·3%; as to λ_6^2, the relative error of the CEM ($1 \times 7c$) scheme is 1·51%, that of the CEM ($2 \times 3c$) scheme is 4·84%, and that of the FEM (8e) scheme already reaches 38·5%; as to λ_4^2, the relative error of the CEM ($1 \times 7c$) scheme is 0·452%, that of the CEM ($2 \times 3c$) scheme is 0·776%, that of the CEM ($4 \times 1c$) scheme is 4·98%, and that of the FEM (8e) scheme already reaches 16·5%; as to λ_1^2, the relative error of the CEM ($1 \times 7c$)

TABLE 1

λ_i^2 of various schemes in case of 1 element discretization

Order	Exact $[(2r-1)\pi/2]^2$	CEM $(1 \times 1c)$* c-DOF:1 Total-DOF:2	CEM $(1 \times 3c)$ c-DOF:3 Total-DOF:4	CEM $(1 \times 7c)$ c-DOF:7 Total-DOF:8	CEM $(1 \times 11c)$ c-DOF:11 Total-DOF:12	CEM $(1 \times 15c)$ c-DOF:15 Total-DOF:16
λ_1^2	2·467401	2·489484	2·469294	2·467595	2·467453	2·467421
λ_2^2	22·20661	30·33504	22·37845	22·22286	22·21105	22·20839
λ_3^2	61·68503		63·47546	61·81663	61·72017	61·69919
λ_4^2	120·9027		171·5595	121·4490	121·0417	120·9579
λ_5^2	199·8595			201·5406	200·2560	200·0142
λ_6^2	298·5555			303·0586	299·4902	298·9100
λ_7^2	416·9908			429·0039	418·9527	417·7069
λ_8^2	555·1652			796·1646	558·9959	556·4908
λ_9^2	713·0789				720·2640	715·3847
λ_{10}^2	890·7318				904·1693	894·5660
λ_{11}^2	1088·124				1114·889	1094·320
λ_{12}^2	1305·255				1875·630	1315·122
λ_{13}^2	1542·126					1557·753
λ_{14}^2	1798·735					1823·968
λ_{15}^2	2075·084					2119·011
λ_{16}^2	2371·172					3409·789

* Note: the symbol CEM $(1 \times 1c)$ of Table 1 means using one CEM element with $1c$-DOF; CEM $(1 \times 11c)$ means using one CEM element with $11c$-DOF, and so on.

scheme is 0·0078%, that of the CEM ($2 \times 3c$) scheme is 0·014%, that of the CEM ($4 \times 1c$) scheme is 0·021%, and that of the FEM (8e) scheme already reaches 0·32%.

(5) *Effect of allocation of c-DOF*

We consider the case of total-DOF = 12 and total c-DOF = 8 when using 4 CEM elements. If total-DOF (=12) and total c-DOF (=8) are fixed in various computational schemes, we investigate the effect of allocation of c-DOF on results. For example, the scheme CEM ($4 \times 2c$) uses 4 CEM elements, each having $2c$-DOF; the scheme CEM ($3c1c3c1c$) uses 4 CEM elements: the first element takes $3c$-DOF, the second element takes $1c$-DOF, the third element takes $3c$-DOF and the fourth element takes $1c$-DOF; and the schemes CEM ($1c3c1c3c$), CEM ($4c0c4c0c$), CEM ($0c4c0c4c$) have a similar representation. All these schemes have a common feature: total-DOF = 12, total c-DOF = 8. The calculated results and comparisons between them are presented in Table 5.

The results in Table 5 show that the schemes with even allocation of c-DOF is obviously superior to other schemes. The reason lies in that c-DOF is a very important aspect of describing the displacement field and any partly absent and poor allocation of c-DOF will reduce the ability of c-DOF. A discussion on c-version will further present some more details on this aspect later.

4.2. COMPARISONS BETWEEN COMPOSITE ELEMENT METHOD AND FEM

We will compare the Composite Element Method and FEM from two aspects of h-version and c-version. Below all comparisons are symbolized by the computation effort, i.e., total-DOF.

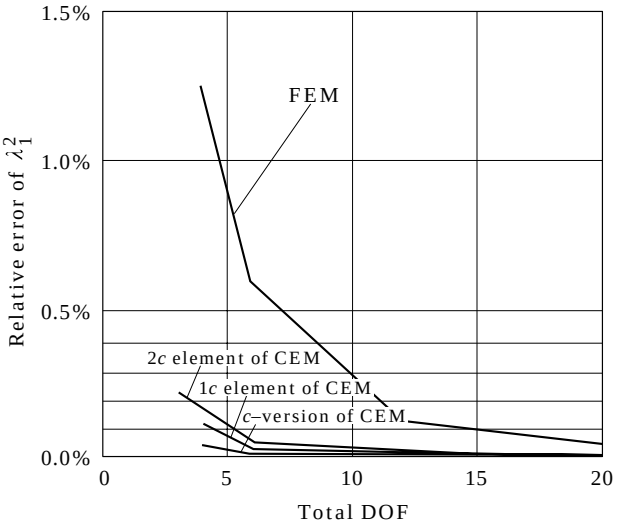

Figure 5. The relative errors of the 1st-order eigenvalue for a clamped-free rod.

(1) *h-version*

The *h*-version of the Composite Element Method is completely similar to one of FEM, i.e., improving the accuracy by refining the element mesh. In the cases of using the 1*c*-DOF composite element and the 2*c*-DOF composite element, we present the detailed results of *h*-version in Tables 6 and 7 respectively.

- **1*c* element**

In the case of using the 1*c*-DOF composite element, for a clamped-free rod shown in Figure 4, we consider the following schemes: when total-DOF is assigned as 6, three 1*c*-DOF elements (i.e., CEM ($3 \times 1c$) and 6 FEM elements (i.e., FEM (6e)) are used; when total-DOF is assigned as 12, six 1*c*-DOF elements (i.e., CEM ($6 \times 1c$)) and 12 FEM elements (i.e., FEM (12e)) are used; when total-DOF is assigned as 18, using nine 1*c*-DOF elements (i.e., CEM ($9 \times 1c$)) and 18 FEM elements (i.e., FEM (18e)) are used. All results are listed in Table 6. Relative errors are shown in Figures 5–8.

- **2*c* element**

In the case of using the 2*c*-DOF composite element, for a clamped-free rod shown in Figure 4, we consider the following schemes: when total-DOF is assigned as 6, two 2*c*-DOF elements (i.e., CEM ($2 \times 2c$)) and 6 FEM elements (i.e., FEM (6e)) are used; when total-DOF is assigned as 12, four 2*c*-DOF elements (i.e., CEM ($4 \times 2c$)) and 12 FEM elements (i.e., FEM (12e)) are used; when total-DOF is assigned as 18, six 2*c*-DOF elements (i.e., CEM ($6 \times 2c$)) and 18 FEM elements (i.e., FEM (18e)) are used. All results are listed in Table 7. Relative errors are shown in Figures 5–8.

(2) *c-version*

Previously, many numerical results of increasing the *c*-DOF have shown high efficiency and good approximation of the CEM on eigenvalues, especially for higher-order eigenvalues (see Tables 2–5). Now, also for a clamped-free rod shown in Figure 4, we present a more detailed comparison of the *c*-version of the Composite Element Method with the conventional FEM. The numerical results are listed in Table 8 and the relative error curves are shown in Figures 5–8. The *c*-version of the Composite Element Method can lead to a superconvergence for computing the eigenvalues of a structure, especially for higher-order eigenvalues. For instance, for λ_1^2, the result (total-DOF = 4) of the *c*-version of the Composite Element Method will nearly correspond to that (total-DOF = 18) of the FEM; for λ_4^2, the result (total-DOF = 6) of the *c*-version of the Composite Element Method will be better than that (total-DOF = 18) of the FEM; for higher-order eigenvalue λ_{15}^2, the relative error of *c*-version (total-DOF = 18) is only 0·998%, but the relative error of FEM (total-DOF = 18) already reaches 44·3%.

4.3. COMMENTS

From the numerical results above, we can sum up some features of the *h*-version and *c*-version of the Composite Element Method as follows.

(1) The *c*-DOF of CEM has a powerful potential to improve the accuracy of analysis. Therefore, in choosing the trial function of displacement field, increasing the number of *c*-DOF and decreasing the number of nodal DOF of element will

TABLE 2

λ_i^2 of various schemes in case of 2 elements discretization

Order	Exact $[(2r-1)\pi/2]^2$	FEM (2e)* c-DOF:0 Total-DOF:2	CEM ($2 \times 1c$) c-DOF:2 Total-DOF:4	CEM ($2 \times 3c$) c-DOF:6 Total-DOF:8	CEM ($2 \times 5c$) c-DOF:10 Total-DOF:12	CEM ($2 \times 7c$) c-DOF:14 Total-DOF:16
λ_1^2	2·467401	2·596660	2·470240	2·467743	2·467500	2·467441
λ_2^2	22·20661	31·68905	22·93332	22·25608	22·21854	22·21113
λ_3^2	61·68503		75·28844	62·09487	61·77947	61·72043
λ_4^2	120·9027		171·8927	121·8409	121·1581	120·0070
λ_5^2	199·8595			202·8309	200·5933	200·1522
λ_6^2	298·5555			313·0020	301·0986	299·4468
λ_7^2	416·9908			554·5635	422·7410	418·8356
λ_8^2	555·1652			818·6693	561·8766	557·6293
λ_9^2	713·0789				726·9096	717·5087
λ_{10}^2	890·7318				926·9652	900·4362
λ_{11}^1	1088·124				1490·646	1105·945
λ_{12}^2	1305·255				1918·361	1322·451
λ_{13}^2	1542·126					1573·939
λ_{14}^2	1798·735					1859·524
λ_{15}^2	2075·084					2883·516
λ_{16}^2	2371·172					3474·304

* Note: the symbol FEM (2e) of the Table 2 denotes using 2 bar elements of the conventional FEM, CEM ($2 \times 3c$) means using 2 CEM elements with $3c$-DOF each.

significantly improve the accuracy for dynamic analysis of a structure. Meanwhile, in the case of multi-discretization elements, the scheme with the even allocation of the c-DOF for each element is superior to other schemes.

(2) The convergence of the h-version and the c-version of the composite element is obviously superior to that of conventional FEM. With less computation effort, both the h-version and the c-version of CEM can approximate the desired solution. Usually, against the computational effort, the error of CEM is one order of magnitude less than that of the conventional FEM.

(3) For lower order eigenvalues, both the h-version and the c-version of the CEM can lead to a superconvergence, although the c-version of CEM is superior to the h-version of CEM. It means that, with only few c-DOF, the Composite Element Method can obtain a good result. For higher order eigenvalues, only the c-version of the Composite Element Method can continue to lead to a superconvergence.

5. APPLICATIONS

5.1. VIBRATION ANALYSIS OF 7 BAR TRUSS

Let us consider the case of a structure made of 7 bars [24] shown in Figure 9, and find the natural frequencies and modes of free vibration. The members are hinged at joints in such a way that they contribute to the global stiffness only

TABLE 3

λ_i^2 of various schemes in case of 4 elements discretization

Order	Exact $[(2r-1)\pi/2]^2$	FEM (4e)* c-DOF:0 Total-DOF:4	CEM ($4\times 1c$) c-DOF:4 Total-DOF:8	CEM ($4\times 2c$) c-DOF:8 Total-DOF:12	CEM ($4\times 3c$) c-DOF:12 Total-DOF:16
λ_1^2	2·467401	2·499269	2·467922	2·467850	2·467470
λ_2^2	22·20661	24·87211	22·28786	22·23677	22·21473
λ_3^2	61·68503	82·07272	62·81638	61·84864	61·77038
λ_4^2	120·9027	171·6279	126·9223	121·3352	121·2966
λ_5^2	199·8595		233·6277	201·1083	200·9905
λ_6^2	298·5555		384·9870	303·0808	300·7531
λ_7^2	416·9908		598·5134	431·7375	420·2496
λ_8^2	555·1652		799·6738	585·2877	559·4969
λ_9^2	713·0789			898·5939	721·1412
λ_{10}^2	890·7318			1198·133	909·1962
λ_{11}^2	1088·124			1582·031	1130·756
λ_{12}^2	1305·255			1893·178	1365·497
λ_{13}^2	1542·126				2024·445
λ_{14}^2	1798·735				2467·178
λ_{15}^2	2075·084				3025·804
λ_{16}^2	2371·172				3449·116

* Note: the symbol FEM (4e) of the Table 3 denotes using 4 bar elements of the conventional FEM, CEM ($4\times 1c$) means using 4 CEM elements with $1c$-DOF each, and so on.

TABLE 4

λ_i^2 of various schemes in case of total-DOF = 8

Order	Exact $[(2r-1)\pi/2]^2$	CEM ($1 \times 7c$) c-DOF:7 Total-DOF:8	CEM ($2 \times 3c$) c-DOF:6 Total-DOF:8	CEM ($4 \times 1c$) c-DOF:4 Total-DOF:8	FEM (8e) c-DOF:0 Total-DOF:8
λ_1^2	2·467401	2·467595	2·467743	2·467922	2·475339
λ_2^2	22·20661	22·22286	22·25608	22·28786	22·85585
λ_3^2	61·68503	61·81663	62·09487	62·81638	66·78001
λ_4^2	120·9027	121·4490	121·8409	126·9223	140·8074
λ_5^2	199·8595	201·5406	202·8309	233·6277	254·2591
λ_6^2	298·5555	303·0586	313·0020	384·9870	413·5462
λ_7^2	416·9908	429·0039	554·5638	598·5134	601·8537

through their extension stiffness. The related data are as follows: span $L = 2l = 4$ m, height $h = 2$ m, cross-section area $A = 0{\cdot}001$ m^2, density $\rho = 8000$ Ns^2/m^4, Young's modulus $E = 2{\cdot}1 \times 10^{11}$ N/m^2.

First, we consider the case of an element making an angle γ with the x axis [Figure 9(b)]. Passing from the local axial displacements $[q_i\, q_j]$ to the global displacements, $[u_i\, v_i\, u_j\, v_j]$ is expressed by the transformation

$$q_i = u_i \cos\gamma + v_i \sin\gamma \tag{51}$$

$$q_j = u_j \cos\gamma + v_j \sin\gamma. \tag{52}$$

If we use the composite element, the transformation relations between the local coordinate δ^e and the global coordinate $\overline{\delta}^e$ is expressed as

$$\delta^e = \mathbf{T}^e \overline{\delta}^e \tag{53}$$

where

$$\delta^e = [q_i \quad q_j \quad c_1 \quad c_2 \quad \cdots \quad c_n]^{\mathrm{T}} \tag{54}$$

$$\overline{\delta}^e = [u_i \quad v_i \quad u_j \quad v_j \quad c_1 \quad c_2 \quad \cdots \quad c_n]^{\mathrm{T}} \tag{55}$$

$c_1, c_2, \ldots, c_n$ are the c-DOF (c-coordinate).

(1) *Assembled stiffness and mass matrices*

$$\mathbf{K} = \sum_{e=1}^{7} \mathbf{K}^{(e)}$$

$$= EA \cdot \begin{array}{c} \begin{array}{ccccccc} u_2 & v_2 & u_3 & v_3 & u_4 & v_4 & c \end{array} \\ \left[\begin{array}{ccccccc|c} \frac{1}{2}+\frac{2}{5\sqrt{5}} & & & & & & & u_2 \\ 0 & \frac{8}{5\sqrt{5}} & & & & & & v_2 \\ -\frac{1}{5\sqrt{5}} & \frac{2}{5\sqrt{5}} & 1+\frac{2}{5\sqrt{5}} & & & sym. & & u_3 \\ \frac{2}{5\sqrt{5}} & -\frac{4}{5\sqrt{5}} & 0 & \frac{8}{5\sqrt{5}} & & & & v_3 \\ -\frac{1}{2} & 0 & -\frac{1}{5\sqrt{5}} & -\frac{2}{5\sqrt{5}} & \frac{1}{2}+\frac{2}{5\sqrt{5}} & & & u_4 \\ 0 & 0 & -\frac{2}{5\sqrt{5}} & -\frac{4}{5\sqrt{5}} & 0 & \frac{8}{5\sqrt{5}} & & v_4 \\ \hline & & & & 0 & & \mathbf{K}_{cc} & c \end{array}\right] \end{array} \tag{56}$$

where $\mathbf{K}_{cc}$ is the sub-matrix as follows

$$\mathbf{K}_{cc} = \begin{array}{c} \begin{matrix} c_{11} & c_{12} & c_{21} & c_{22} & c_{31} & c_{32} & c_{41} & c_{42} & c_{51} & c_{52} & c_{61} & c_{62} & c_{71} & c_{72} \end{matrix} \\ \begin{bmatrix} \frac{\pi^2}{2\sqrt{5}} & & & & & & & & & & & & & \\ & \frac{4\pi^2}{2\sqrt{5}} & & & & & & & & & & & & \\ & & \frac{\pi^2}{4} & & & & & & & & & & & \\ & & & \pi^2 & & & & & & & & & & \\ & & & & \frac{\pi^2}{2\sqrt{5}} & & & & & 0 & & & & \\ & & & & & \frac{4\pi^2}{2\sqrt{5}} & & & & & & & & \\ & & & & & & \frac{\pi^2}{4} & & & & & & & \\ & & & & & & & \pi^2 & & & & & & \\ & & & & & & & & \frac{\pi^2}{2\sqrt{5}} & & & & & \\ & & & & 0 & & & & & \frac{4\pi^2}{2\sqrt{5}} & & & & \\ & & & & & & & & & & \frac{\pi^2}{4} & & & \\ & & & & & & & & & & & \pi^2 & & \\ & & & & & & & & & & & & \frac{\pi^2}{2\sqrt{5}} & \\ & & & & & & & & & & & & & \frac{4\pi^2}{2\sqrt{5}} \end{bmatrix} \end{array} \begin{matrix} c_{11} \\ c_{12} \\ c_{21} \\ c_{22} \\ c_{31} \\ c_{32} \\ c_{41} \\ c_{42} \\ c_{51} \\ c_{52} \\ c_{61} \\ c_{62} \\ c_{71} \\ c_{72} \end{matrix} \tag{57}$$

The assembled mass matrix is

$$\mathbf{M} = \sum_{e=1}^{7} \mathbf{M}^{(e)}$$

$$= \rho A \cdot \begin{array}{c} \begin{array}{ccccccc} u_2 & v_2 & u_3 & v_3 & u_4 & v_4 & c \end{array} \\ \left[\begin{array}{ccccccc|c} \frac{2}{3}+\frac{2\sqrt{5}}{15} & & & & & & & u_2 \\ 0 & \frac{8\sqrt{5}}{15} & & & & & & v_2 \\ \frac{\sqrt{5}}{30} & -\frac{2\sqrt{5}}{30} & \frac{4}{3}+\frac{2\sqrt{5}}{15} & & & sym. & & u_3 \\ -\frac{2\sqrt{5}}{30} & \frac{4\sqrt{5}}{30} & 0 & \frac{8\sqrt{5}}{15} & & & sym. & v_3 \\ \frac{1}{3} & 0 & \frac{5\sqrt{5}}{30} & \frac{2\sqrt{5}}{30} & \frac{2}{3}+\frac{2\sqrt{5}}{15} & & & u_4 \\ 0 & 0 & \frac{2\sqrt{5}}{30} & \frac{4\sqrt{5}}{30} & 0 & \frac{8\sqrt{5}}{15} & & v_4 \\ \hline & & & \mathbf{M}_{cq} & & & \mathbf{M}_{cc} & c \end{array}\right] \end{array} \tag{58}$$

where $\mathbf{M}_{cq}$ and $\mathbf{M}_{cc}$ are the sub-matrices as follows

$$\mathbf{M}_{cq} = \begin{array}{c} \begin{matrix} u_2 & v_2 & u_3 & v_3 & u_4 & v_4 \end{matrix} \\ \begin{bmatrix} \frac{1}{\pi} & \frac{2}{\pi} & 0 & 0 & 0 & 0 \\ -\frac{1}{2\pi} & -\frac{1}{\pi} & 0 & 0 & 0 & 0 \\ 0 & 0 & \frac{2}{\pi} & 0 & 0 & 0 \\ 0 & 0 & -\frac{1}{\pi} & 0 & 0 & 0 \\ \frac{1}{\pi} & -\frac{2}{\pi} & \frac{1}{\pi} & -\frac{2}{\pi} & 0 & 0 \\ \frac{1}{2\pi} & -\frac{1}{\pi} & -\frac{1}{2\pi} & \frac{1}{\pi} & 0 & 0 \\ \frac{2}{\pi} & 0 & 0 & 0 & \frac{2}{\pi} & 0 \\ \frac{1}{\pi} & 0 & 0 & 0 & -\frac{1}{\pi} & 0 \\ 0 & 0 & \frac{1}{\pi} & \frac{2}{\pi} & \frac{1}{\pi} & \frac{2}{\pi} \\ 0 & 0 & \frac{1}{2\pi} & \frac{1}{\pi} & -\frac{1}{2\pi} & -\frac{1}{\pi} \\ 0 & 0 & \frac{2}{\pi} & 0 & 0 & 0 \\ 0 & 0 & \frac{1}{\pi} & 0 & 0 & 0 \\ 0 & 0 & 0 & 0 & \frac{1}{\pi} & -\frac{2}{\pi} \\ 0 & 0 & 0 & 0 & \frac{1}{2\pi} & -\frac{1}{\pi} \end{bmatrix} \begin{matrix} c_{11} \\ c_{12} \\ c_{21} \\ c_{22} \\ c_{31} \\ c_{32} \\ c_{41} \\ c_{42} \\ c_{51} \\ c_{52} \\ c_{61} \\ c_{62} \\ c_{71} \\ c_{72} \end{matrix} \end{array} \tag{59}$$

$$
\mathbf{M}_{cc} = \begin{array}{c}
\begin{array}{cccccccccccccccccc}
c_{11} & c_{12} & c_{21} & c_{22} & c_{31} & c_{32} & c_{41} & c_{42} & c_{51} & c_{52} & c_{61} & c_{62} & c_{71} & c_{72}
\end{array} \\
\begin{bmatrix}
\frac{\sqrt{5}}{2} & & & & & & & & & & & & & \\
& \frac{\sqrt{5}}{2} & & & & & & & & & & & & \\
& & 1 & & & & & & & & & & & \\
& & & 1 & & & & & & & & & & \\
& & & & \frac{\sqrt{5}}{2} & & & & & & & & & \\
& & & & & \frac{\sqrt{5}}{2} & & & & & & & & \\
& & & & & & 1 & & & & & & & \\
& & & & & & & 1 & & & & & & \\
& & & & & & & & \frac{\sqrt{5}}{2} & & & & & \\
& & & & 0 & & & & & \frac{\sqrt{5}}{2} & & & & \\
& & & & & & & & & & 1 & & & \\
& & & & & & & & & & & 1 & & \\
& & & & & & & & & & & & \frac{\sqrt{5}}{2} & \\
& & & & & & & & & & & & & \frac{\sqrt{5}}{2}
\end{bmatrix}
\end{array}
\qquad (60)
$$

TABLE 5

λ_i^2 of various schemes in case of total-DOF = 12, total c-DOF = 8

Order	Exact $[(2r-1)\pi/2]^2$	CEM ($4 \times 2c$) c-DOF:8 Total-DOF:12	CEM ($3c1c3c1c$) c-DOF:8 Total-DOF:12	CEM ($1c3c1c3c$) c-DOF:8 Total-DOF:12	CEM ($4c0c4c0c$) c-DOF:8 Total-DOF:12	CEM ($0c4c0c4c$) c-DOF:8 Total-DOF:12	FEM (12e) c-DOF:0 Total-DOF:12
λ_1^2	2·467401	2·467850	2·467737	2·467658	2·487459	2·478897	2·470928
λ_2^2	22·20661	22·23677	22·24173	22·26062	24·26636	22·63271	22·49341
λ_3^2	61·68503	61·84864	62·57712	61·99873	65·34325	75·98917	63·91693
λ_4^2	120·9027	121·3352	124·8778	123·3716	143·2717	147·4531	129·5747
λ_5^2	199·8595	201·1083	217·0603	209·0558	257·7285	328·1271	223·8488
λ_6^2	298·5555	303·0808	353·9830	310·8653	395·6422	486·5539	352·6005
λ_7^2	416·9908	431·7375	461·3058	526·0541	733·6769	835·3319	522·4851
λ_8^2	555·1652	585·2877	672·2731	660·8720	898·8019	1127·907	738·6469

TABLE 6

λ_i^2 of various schemes by h-version using 1c element

		Total-DOF:6		Total-DOF:12		Total-DOF:18	
Order	Exact $[(2r-1)\pi/2]^2$	CEM ($3 \times 1c$) c-DOF:3	FEM (6e)	CEM ($6 \times 1c$) c-DOF:6	FEM (12e)	CEM ($9 \times 1c$) c-DOF:9	FEM (18e)
λ_1^2	2·467401	2·468420	2·481525	2·467616	2·470928	2·467492	2·468963
λ_2^2	22·20661	22·40538	23·36993	22·23213	22·49341	22·21575	22·33370
λ_3^2	61·68503	64·42548	70·87550	61·99640	63·91693	61·77960	62·66967
λ_4^2	120·9027	143·0672	156·1611	122·6776	129·5747	121·3966	124·7070
λ_{10}^2	890·7318			1259·841	1284·098	1033·256	1104·856
λ_{15}^2	2075·084					2964·482	2994·850

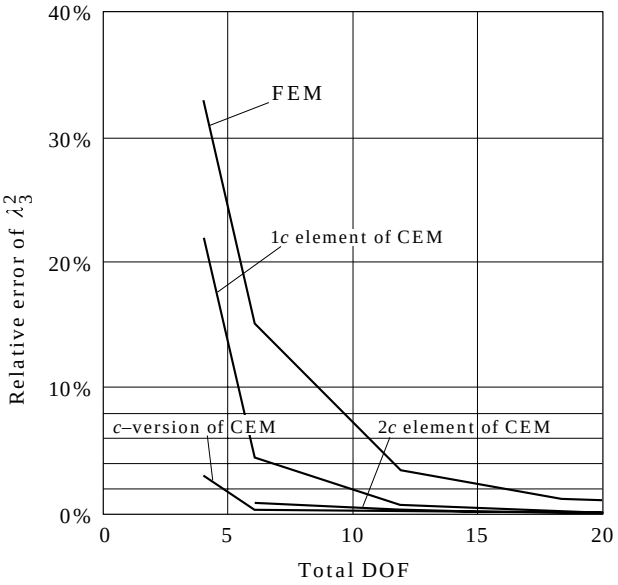

Figure 6. The relative errors of the 3rd-order eigenvalue for a clamped-free rod.

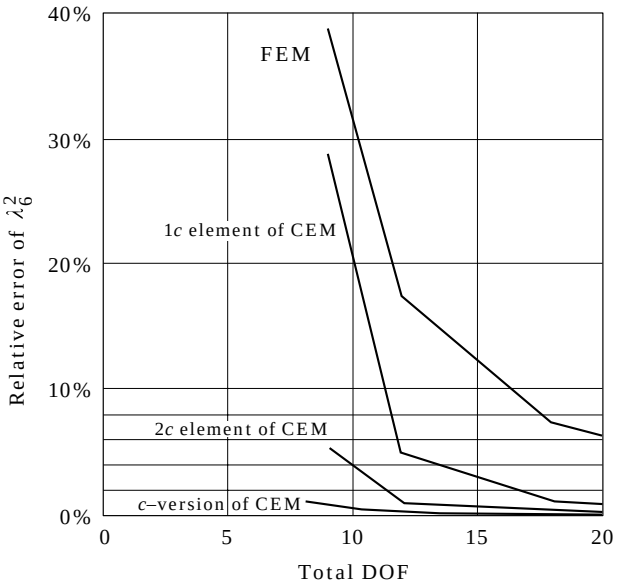

Figure 7. The relative errors of the 6th-order eigenvalue for a clamped-free rod.

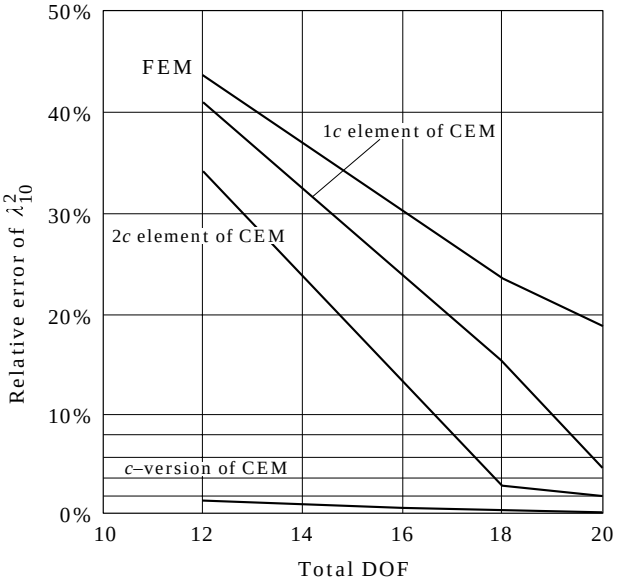

Figure 8. The relative errors of the 10th-order eigenvalue for a clamped-free rod.

(2) *Solution of free vibration equation*

According to the basic equation of free vibration, we have

$$\mathbf{K}\overline{\delta} = \omega^2\mathbf{M}\overline{\delta} \tag{61}$$

where $\overline{\delta}$ is the generalized coordinates of the global system which consists of nodal coordinates of FEM and c-coordinates, i.e.,

$$\overline{\delta} = [u_2 \quad v_2 \quad u_3 \quad v_3 \quad u_4 \quad v_4 \quad c_{11} \quad c_{12} \quad c_{21} \quad c_{22} \quad c_{31} \quad c_{32} \quad c_{41} \quad c_{42} \quad c_{51} \quad c_{52} \quad c_{61} \quad c_{62} \quad c_{71} \quad c_{72}]^{\mathrm{T}}. \tag{62}$$

Substituting equations (56) and (58) into equation (61), we solve equation (61) and obtain the various orders of natural frequencies ω_i, which are compared with the results of the conventional FEM shown in Table 9.

(3) *Natural mode shapes*

Parts of the natural mode shapes are demonstrated in Figures 10–13.

5.2. VIBRATION ANALYSIS OF 15 BAR TRUSS

Let us consider a more complicated truss structure composed of 15 bars [24] shown in Figure 14. The members are hinged at joints in such a way that they contribute to the global stiffness only through their extension stiffness. The basic data are the same as the truss shown in Figure 9, i.e., span $L = 4l = 8$ m, height $h = 2$ m, cross-section area $A = 0{\cdot}001$ m^2, density $\rho = 8000$ Ns^2/m^4, Young's modulus $E = 2{\cdot}1 \times 10^{11}$ N/m^2.

TABLE 7

λ_i^2 of various schemes by h-version using 2c element

Order	Exact $[(2r-1)\pi/2]^2$	Total-DOF:6 CEM ($2\times 2c$) c-DOF:4	Total-DOF:6 FEM (6e)	Total-DOF:12 CEM ($4\times 2c$) c-DOF:8	Total-DOF:12 FEM (12e)	Total-DOF:18 CEM ($6\times 2c$) c-DOF:12	Total-DOF:18 FEM (18e)
λ_1^2	2·467401	2·469072	2·481525	2·467845	2·470928	2·467600	2·468963
λ_2^2	22·20661	22·27573	23·36993	22·23677	22·49341	22·22164	22·33370
λ_3^2	61·68503	62·27393	70·87550	61·84846	63·91693	61·78360	62·66967
λ_4^2	120·9027	126·7798	156·1611	121·3352	129·5747	121·2014	124·7070
λ_{10}^2	890·7318			1198·133	1284·098	918·4833	1104·856
λ_{15}^2	2075·084					2832·317	2994·850

TABLE 8

λ_i^2 of various schemes by c-version

Order	Exact $[(2r-1)\pi/2]^2$	Total-DOF:4 CEM ($1\times 3c$) c-DOF:3	Total-DOF:4 FEM (4e)	Total-DOF:6 CEM ($1\times 5c$) c-DOF:5	Total-DOF:6 FEM (6e)	Total-DOF:12 CEM ($1\times 11c$) c-DOF:11	Total-DOF:12 FEM (12e)	Total-DOF:18 CEM ($1\times 17c$) c-DOF:17	Total-DOF:18 FEM (18e)
λ_1^2	2·467401	2·469294	2·499269	2·467896	2·481525	2·467453	2·470928	2·467413	2·468963
λ_2^2	22·20661	22·37845	24·87211	22·24848	23·36993	22·21105	22·49341	22·20784	22·33370
λ_3^2	61·68503	63·47546	82·07272	62·04041	70·87550	61·72017	63·91693	61·69481	62·66967
λ_4^2	120·9027			122·5219	156·1611	121·0417	129·5747	120·9407	124·7070
λ_{10}^2	890·7318					904·1693	1284·098	893·2147	1104·856
λ_{15}^2	2075·084							2095·796	2994·850

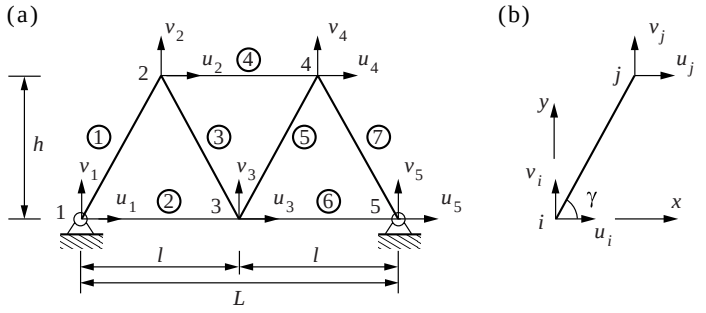

Figure 9. 7-bar structure.

The analysis procedure for this truss by the Composite Element Method is completely similar to the above example. Therefore, we will focus on the analyses and comparisons of results.

(1) *Natural frequencies*

We take 1c-DOF and 2c-DOF for each element of truss, then compare the calculated natural frequencies with the results of FEM, which are shown in Table 10.

(2) *Natural mode shapes*

Parts of the natural mode shapes of the 15-bar truss structure are shown in Figures 15–17.

(3) *Comments*

The results of Tables 9 and 10 show us that the CEM can obtain higher-accuracy natural frequencies than the conventional FEM, especially for higher-order

TABLE 9

Various orders of ω_i *by CEM* (7 × 2c), *CEM* (7 × 1c) *and FEM*

Order	By CEM (7 × 2c) (Hz) c-DOF:14 Total-DOF:20	By CEM (7 × 1c) (Hz) c-DOF:7 Total-DOF:13	By FEM (Hz) Total-DOF:6
ω_1	1648·26	1648·52	1683·52
ω_2	1741·32	1741·66	1776·28
ω_3	3113·83	3119·12	3341·37
ω_4	4567·69	4600·60	5174·35
ω_5	4829·70	4870·58	5678·18
ω_6	7379·96	7380·83	8315·40
ω_7	7532·30	8047·93	
ω_8	8047·93	8272·61	
ω_9	9997·48	11167·57	
ω_{10}	10567·43	12051·90	
ω_{11}	12282·63	14359·31	
ω_{12}	13296·29	15525·68	
ω_{13}	13654·89	16792·68	

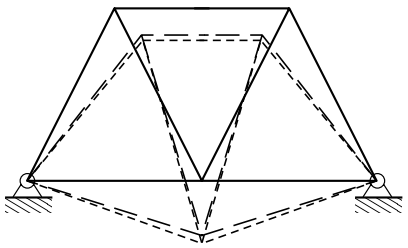

Figure 10. The first-order natural mode of 7-bar truss. — — —, by CEM ($7 \times 2c$); ---, by FEM; $\omega_{1CEM} = 1648{\cdot}26$ Hz; $\omega_{1FEM} = 1683{\cdot}52$ Hz.

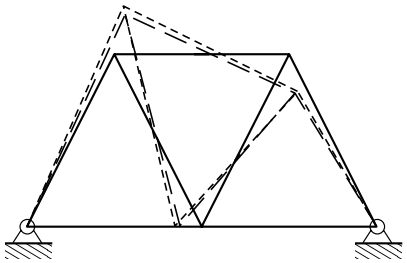

Figure 11. The 3rd-order natural mode of 7-bar truss. — — —, by CEM ($7 \times 2c$); ---, by FEM; $\omega_{3CEM} = 3113{\cdot}83$ Hz; $\omega_{3FEM} = 3341{\cdot}37$ Hz.

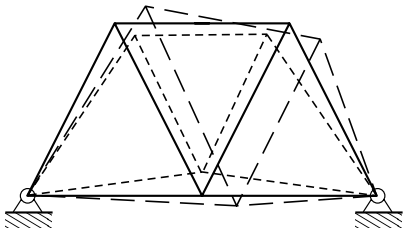

Figure 12. The 6th-order natural mode of 7-bar truss. — — —, by CEM ($7 \times 2c$); ---, by FEM; $\omega_{6CEM} = 7379{\cdot}96$ Hz; $\omega_{6FEM} = 8315{\cdot}40$ Hz.

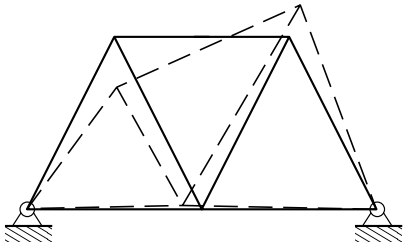

Figure 13. The 10th-order natural mode of 7-bar truss. — — —, by CEM ($7 \times 2c$); ---, by FEM; $\omega_{10CEM} = 10\ 567{\cdot}43$ Hz.

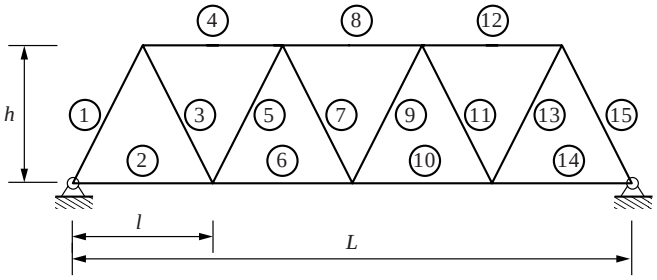

Figure 14. 15-bar truss.

frequencies. For instance, as to ω_1 of the 7-bar truss, the relative error between CEM and FEM is 2·14%; as to ω_3, 7·31%; as to ω_6, 12·7%. For the 15-bar truss, as to ω_1, the relative error between CEM and FEM is 0·36%; as to ω_6, 5·43%; as to ω_{14}, 14·7%. The natural mode configurations shown in Figures 15–17 also reflect the difference in the results between the CEM and the FEM, i.e., for lower-order modes, the error between them is not large, but, for higher-order modes, the error is obvious.

TABLE 10

Various orders of ω_i by CEM (15 × 2c), CEM (15 × 1c) and FEM

Order	By CEM (15 × 2c) (Hz) c-DOF:30 Total-DOF:44	By CEM (15 × 1c) (Hz) c-DOF:15 Total-DOF:29	By FEM (Hz) Total-DOF:14
ω_1	679·82	679·82	682·27
ω_2	1139·34	1139·38	1149·30
ω_3	1582·18	1582·39	1612·35
ω_4	2410·25	2411·84	2519·87
ω_5	2601·85	2604·12	2715·76
ω_6	2815·44	2818·30	2968·22
ω_7	3293·26	3300·49	3573·36
ω_8	3811·37	3824·74	4207·78
ω_9	4480·52	4507·65	5134·74
ω_{10}	4707·91	4746·38	5399·56
ω_{11}	6069·27	6189·38	7163·28
ω_{12}	6341·62	6493·48	7471·07
ω_{13}	6455·52	6623·73	7586·07
ω_{14}	7381·06	7386·07	8462·58
ω_{15}	7604·45	8047·93	
ω_{16}	8047·93	8319·71	
ω_{17}	8325·93	8986·32	
ω_{18}	8771·85	9487·92	
ω_{19}	9578·30	10492·01	
ω_{20}	10257·94	11570·63	

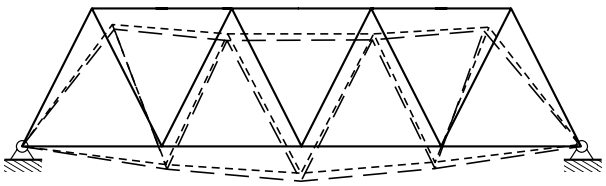

Figure 15. The first-order natural mode of 15-bar truss. — — —, by CEM ($7 \times 2c$); ---, by FEM; $\omega_{1CEM} = 679{\cdot}82$ Hz; $\omega_{1FEM} = 682{\cdot}27$ Hz.

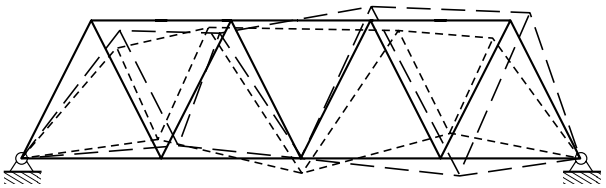

Figure 16. The 14th-order natural mode of 15-bar truss. — — —, by CEM ($7 \times 2c$); ---, by FEM; $\omega_{14CEM} = 7381{\cdot}06$ Hz; $\omega_{14FEM} = 8462{\cdot}58$ Hz.

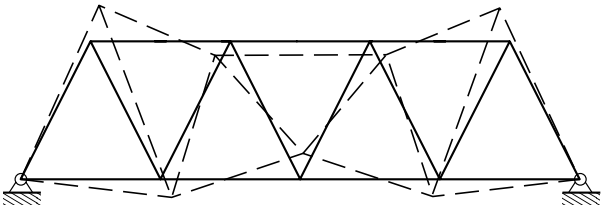

Figure 17. The 20th-order natural mode of 15-bar truss. — — —, by CEM ($7 \times 2c$); ---, by FEM; $\omega_{20CEM} = 10\,257{\cdot}94$ Hz.

6. REMARKS

It has been noted that the conventional FEM possesses some excellent characteristics such as extreme versatility and effectiveness for solving elliptic differential equations. Moreover, the classical theory can supply the exact or near-exact analytical solution to some regular components, such as longitudinal bar, torsional shaft, bending beam, etc., under simple boundary conditions. This paper has addressed the possibility of combination of these two methods by the Rayleigh–Ritz principle, resulting in developing a new numerical approach for structural dynamics: Composite Element Method. The related characteristics and convergency of CEM are summarized as follows.

(1) As has been said above, Composite Element Method is proposed by combining the conventional FEM and classical theory, and therefore, theoretically speaking, it inherits the typical characteristics of the FEM and classical theory, i.e., powerful versatility of the FEM in dealing with various complex geometric shapes and boundary conditions, and the excellent approximation and superconvergency of the classical theory.

(2) The core of CEM is to choose a special combined function as the trial function of a displacement field, which consists of two parts: the nodal interpolation polynomials of the FEM and a series of analytical solutions under the zero-boundary condition using the classical theory. The series of the combined trial functions are also admissible, so that they can be used within the Rayleigh–Ritz principle. Meanwhile the requirement for completeness and compatibility can be entirely satisfied if the interpolation polynomials of the displacement field of the FEM can guarantee it. Actually, the longitudinal bar element, the torsional shaft element and the bending beam element in CEM to be developed later are complete and compatible.

(3) In order to get a more accurate solution, two approaches are available to improve CEM, the h-version and the c-version. Without any exception, the h-version of CEM just like that of FEM is to refine the element mesh. However, the c-version of CEM is defined as increasing of the c-DOF (i.e., increasing the trial function terms obtained from the analytical solution of the classical theory), which is not similar to the p-version of the conventional FEM. A large number of numerical examples show the c-version of CEM is of paramount significance in obtaining the fine approximate solution in structural dynamics.

(4) It can be found that a superconvergence appears in CEM to solve structural dynamical problems. The reason lies in that the trial function used in CEM involves a set of hierarchical analytical bases obtained from the classical theory, instead of the usual polynomial bases. It means that the trial functions already inherently include the properties of various modes of components. The c-version is, in some sense, related to the theory of spectral method. Therefore, the use of the c-version of CEM results in achieving an improved approximate solution for less computational effort than the use of mesh refinement.

ACKNOWLEDGMENT

This Project 59775017 is supported by National Natural Science Foundation of China. Also, the work involved in the paper is supported by Alexander von Humboldt Foundation of Germany and Doctoral Dissertation Foundation of Tsinghua University.

REFERENCES

1. O. C. Zienkiewicz and B. Morgan 1983 *Finite Elements and Approximation*. New York: Wiley.
2. O. C. Zienkiewicz and A. W. Craig 1983 *Adaptive Computational Methods for Partial Differential Equations* (Babuska, Chandra and Flaherty, editors) 33–56. Adaptive mesh refinement and *a posteriori* error estimation for the p-version of the FEM.
3. A. G. Peano 1976 *Computers and Mathematics with Applications* **2**, 211–224. Hierarchies of conforming finite elements for plane elasticity and plate bending.
4. L. Meirovitch and H. Bahruh 1983 *International Journal for Numerical Methods in Engineering* **19**, 281–291. On the inclusion principle for hierarchical finite element method.

5. N. S. BARDELL 1991 *Structural Dynamics: Recent Advances* (M. Petyt, H. F. Wolfe and C. Mei, editors), Oxford: Elsevier Applied Science, 221–230. Free vibration analysis of a flat plate using the hierarchical finite element method.
6. N. S. BARDELL 1991 *Structural Dynamics: Recent Advances* (M. Petyt, H. F. Wolfe and C. Mei, editors), Oxford: Elsevier Applied Science, 254–263. The free vibration of cylindrically curved rectangular panels.
7. S. TIMOSHENKO, D. H. YOUNG and W. WEAVER 1974 *Vibration Problems in Engineering*. New York: Wiley.
8. P. DUNNE 1968 *Aeronautical Journal* **72**, 245–246. Complete polynomial displacement fields for the finite element method.
9. F. M. L. AMIROUCHE 1992 *Computational Methods in Multibody Dynamics*. Englewood Cliffs, NJ: Prentice–Hall.
10. O. C. ZIENKIEWICZ and R. L. TAYLOR 1989 *The Finite Element Method*. New York: McGraw-Hill.
11. S. S. RAO 1989 *The Finite Element Method in Engineering*. Oxford: Pergamon Press.
12. D. MCHENRY 1943 *J. Inst. Civ. Eng*. **21**, 59–82. A lattice analogy for the solution of plane stress problems.
13. A. HRENIKOFF 1941 *J. Appl. Mech*. **A8**, 169–175. Solution of problems in elasticity by the framework method.
14. N. M. NEWMARK 1949 *Numerical Methods in Analysis in Engineering* (L. E. Grinter, editor). Oxford: Macmillan. Numerical methods of analysis in bars, plates and elastic bodies.
15. J. H. ARGYRIS 1960 *Energy Theorems and Structural Analysis*. London: Butterworth.
16. M. J. TURNER, R. W. CLOUGH, H. C. MARTIN and L. J. TOPP 1956 *J. Aero. Sci*. **23**, 805–823. Stiffness and deflection analysis of complex structures.
17. R. W. CLOUGH 1960 *Proc. 2nd ASCE Conf. on Electronic Computation*, Pittsburgh. The finite element in plane stress analysis.
18. O. C. ZIENKIEWICZ and J. Z. ZHU 1991 *Computational Mechanics* (Y. K. Cheung, J. H. W. Lee and A. Y. T. Leung, editors), Rotterdam; Balkema, 3–12. Accuracy and adaptivity in FE analysis: The changing face of practical computations.
19. I. BABUSKA, A. MILLER and M. VOGELIUS 1988 *Adaptive Computational Methods for Partial Differential Equations* (Babuska, Chandra and Flaherty, editors), 33–56. SIAM. Adaptive methods and error estimation for elliptic problems of structural mechanics.
20. M. KRIZEK 1994 *Comput. Methods Appl. Mech. Engng* **116**, 157–163. Superconvergence phenomena in the finite element method.
21. J. T. ODEN and A. PATRA 1995 *Comput. Methods Appl. Mech. Engng* **121**, 449–470. A parallel adaptive strategy for *h–p* finite element computations.
22. C. MESZTENYI and A. W. SZYMCZAK 1982 *Tech. Note BN-991*. FEARS User's Manual for UNIVAC 1100, IPST, University of Maryland, College Park.
23. R. E. BANK 1985 *Tech. Report*, Department of Mathematics, University of UCSD. PLTMG User's Guide, Edition 4.0.
24. J. ARGYRIS 1991 *Dynamics of Structures*. Amsterdam: North-Holland.